Muehlberger

The Surface Electrical Properties Experiment

Gene Simmons,[1] David W. Strangway,[2]
L. Bannister,[3] D. Cubley,[4]
G. LaTorraca,[1] J. D. Redman,[5] J. Rossiter,[6]
and R. Watts[6]

Abstract

The surface electrical properties experiment is presently planned for Apollo 17. It uses two orthogonal, electric dipole antennas laid on the surface, each 70 m long (tip-to-tip), to transmit frequencies of 1, 2.1, 4, 8.1, 16 and 32.1 mhz. The signals are received by three mutually perpendicular coils mounted on the lunar Rover which traverses away from the transmitter. Information from the Rover navigation system is also recorded so that it will be possible to construct profiles of each frequency as a function of distance from the transmitter and for each transmitter and each receiving coil. Interferences between waves propagating just above and just below the surface will give a measure of the dielectric constant and loss tangent of the upper layers. Reflections from layers or from lateral inhomogeneities can also be detected and studied.

---

[1]Department of Earth and Planetary Sciences, M.I.T., Cambridge, Mass. 02139

[2]Geophysics Branch, NASA-Manned Spacecraft Center, Houston, Texas 77058

[3]Laboratory for Space Experiments, Center for Space Research, M.I.T. Cambridge, Mass. 02139

[4]Engineering and Development Directorate, NASA-Manned Spacecraft Center, Houston, Texas 77058

[5]Department of Physics, University of Toronto, Toronto, Canada

[6]Dept. of Physics, University of Toronto, Toronto, Canada and Lunar Science Institute, Houston, Texas 77058

A prototype of the system has been constructed and tested on the Athabasca glacier. Analysis of the results show that at 32 mhz, 16 mhz and 8 mhz scattering dominates the results suggesting that scattering bodies of 35 meters or less in size are numerous. At 4 mhz, the ice was found to have a dielectric constant of about 3.3 and a loss tangent of 0.10, both values typical for ice. The depth of the ice was found to be around 275 meters, a value typical for this glacier. At 2 mhz and 1 mhz the losses are much higher following roughly an inverse relation with frequency, and the dielectric constant is determined as $3.3 \pm .2$.

Introduction

The purpose of this paper is to describe the general nature of the Surface Electrical Properties experiment now planned for the Apollo 17 missions. This experiment has been designed specifically to operate in the lunar environment where there is believed to be essentially no moisture present. Electromagnetic experiments on the earth have a long history in the exploration for minerals, but because of the presence of moisture in the pore spaces in rocks it is rare to find conductivities less than about 2×10^{-5} mho/m on earth. The net result of this is that almost all work on the earth has concentrated on using audio frequencies to get significant depths of penetration. The response parameter for electromagnetic waves is given as $(\varepsilon\mu\omega^2 + i\sigma\mu\omega)^{1/2}$ where

ε - dielectric constant - farads/m.

μ - magnetic permeability - henries/m.

ω - rotational frequency ($\omega = 2\pi f$, f - frequency in hz)

σ - conductivity - mhos/m.

For most earth applications $\sigma\mu\omega >> \varepsilon\mu\omega^2$ so that the problem becomes entirely one of diffusion and no propagation takes place. In environments where the resistivity is very high, however, $\varepsilon\mu\omega^2 >> \sigma\mu\omega$ and the problem becomes one of propagation with all the attendant phenomena of diffraction, interference, etc. Early attempts to use radio frequencies to penetrate the earth met with little success, simply because the penetration depth (given by $\sqrt{\frac{2}{\sigma\mu\omega}}$ for the diffusive case and $\frac{\pi f \sqrt{K.\ \tan\delta}}{3 \times 10^8}$ for the propagation case where K = relative dielectric constant and tan δ = loss tangent) was too small. In recent years, experiments on glaciers have

shown that it is possible to get radio-frequency reflections from very great depths (Rinker and Mock, 1967, Harrison, 1970) and radar has been used to map the outline of salt domes (Unterberger et al., 1970, Holser et al., 1970). The reason for success in penetrating significant distances in these two media is that they both have very low conductivities, on the order of 10^{-6} mho/m or less. Lunar soils and rocks have been shown to have very low values of conductivity and accordingly it would appear that the lunar environment is particularly suited to depth sounding using radio frequencies (Strangway, 1969, St. Amant and Strangway, 1970, Katsube and Collett, 1971, Chung et al., 1971).

The properties of typical dielectrics have been reviewed by many workers but in the range of interest to us, the dielectric constant ranges from about 2.5 for powders to about 15 for solids. Equally important is the general phenomenon that the loss tangent is nearly independent of frequency provided there are no relaxations. This was indeed found to be the case for the lunar samples (Katsube and Collett, 1971, Chung, 1972, Strangway et al., in press) so that the lunar materials behave precisely like those earth rocks which have no hydrous minerals (St. Amant and Strangway, 1970). The loss tangent may be converted to a variety of equivalent parameters. Since it is a measure of the imaginary part of the dielectric constant it is also a measure of the real part of the conductivity ($\tan \delta = \frac{K\omega}{\sigma_{app.}}$ where $\sigma_{app.}$ is an apparent conductivity). If there is a finite conductivity, however, this can be converted to an equivalent penetration depth ($\sqrt{\frac{2}{\sigma_{app.}\mu\omega}}$). For a frequency-independent loss tangent this relation is illustrated in Figure 1. Typically, the lunar rocks have values of $\sqrt{K \tan \delta}$ of about

0.05 to about 0.2 and the soils have values which are considerably less. At 1 megahertz the penetration depth in lunar materials is typically a few kilometers while at 30 mhz it is typically a few hundred meters.

The experimental results to be discussed in this paper were measured on glaciers which is almost the only environment on earth in which a suitable analogue experiment can be conducted. The analogy is not excellent, since ice has a relaxation loss that occurs in the audio frequency part of the spectrum. The tail of this relaxation spectrum still affects the loss tangent in the range of frequencies of importance in the surface electrical properties experiment with the result that the loss tangent decreases from 1 mhz to 32 mhz (Evans, 1965) in such a way that the product f. tan δ is approximately constant. The precise value is temperature-dependent, but typically it has values of around 0.2 to 0.5 if the frequency, f, is given in mhz. This effect is illustrated schematically in Figure 1: the attenuation depth in ice, is essentially frequency-independent with a value of a few 100 meters. Ice therefore, is not an optimum analogue for what we expect in the lunar case, but at least it is fairly transparent over part of the frequency range and gives us an opportunity to exercise the system.

Experiment Concept

The concept of the SEP experiment is illustrated in Figure 2. An electric dipole transmitter is laid on the surface and transmits frequencies ranging between 1 mhz and 32 mhz. Energy is propagated in three ways: a) above the surface with the speed of light, b) below the surface along the interface with the velocity of the medium and c) by reflection from

layering or other inhomogeneities in the subsurface. These various waves may interfere with each other as a function of position along the surface. Interference between the surface and subsurface wave gives a measure of the dielectric constant according to the formula $\varepsilon = (1 + \Delta K)^2$ where ΔK is the interference frequency. The rate of decay of the interferences gives a measure of the loss tangent. The receiver is mounted on the Rover and measures the field strength as a function of range so that the interference frequency can be measured. In addition, reflections from subsurface features can be detected as they interfere with the other waves. Transmission is done sequentially from a pair of orthogonal dipoles and the receiver consists of three orthogonal loops to measure the field strength of three independent components.

Instrumentation

Detailed descriptions of the experiment hardware are planned for future papers so we will give only a brief description of the hardware in this section.

The transmitter is powered by solar cells and transmits in a pre-determined sequence at 1, 2.1, 4, 8.1, 16 and 32.1 mhz, each transmission at each frequency from one antenna lasting for 101.25 m seconds. Each frequency is transmitted alternately on a pair of orthogonal dipoles each of which is 70 m long (tip-to-tip). These dipoles are half-wave dipoles at 2.1, 4, 8.1, 16 and 32.1 mhz. A pair of wires is used for the experiment and a set of traps and supressors are built into the wires to give the transmitter the appearance of a half-wave resonant dipole at each of the

frequencies. At 1 mhz the dipole is no longer a half-wave dipole and the transmitting antenna is loaded to compensate for this. Precise matching of the antenna at the dielectric interface is a complicated problem but the choice of a dielectric constant of 3.3 for the lunar surface case has been made,in line with the bistatic radar results of Howard and Tyler (1972). On the ice, the antenna can be adjusted to make the antenna optimum at each frequency. The power transmitted is 3.75 watts at 1 mhz and 2.0 watts at the other frequencies, although only a fraction of this is actually radiated. Transmission is done in the sequence shown in Figure 3 which provides about 10 samples per wavelength per component at 2.1, 4, 8.1, 16 and 32.1 mhz and 20 samples per wavelength per component at 1 mhz at a vehicle speed of 8 km/hr.

The receiver consists of three orthogonal coils which are mounted on the Rover. The reception of each coil is examined in sequence, looking at each coil for 33 msecs. The signals are demodulated in the receiver and are frequency-coded by a voltage controlled oscillator. This oscillator operates over the frequency range of 300 to 3000 hz, corresponding to a dynamic range in the instrument of -35 dbm to -135 dbm. This large dynamic range allows accurate field strength recording over a broad distance range from the transmitter. The voltage-controlled oscillator signal is recorded on a recoverable tape recorder. With six transmitted frequencies, two alternate transmitting antennas and three receiving antennas we record a total of 36 separate pieces of information.

In the lunar system, navigation data will be recorded in two different ways. On each wheel there is a pulse generated every 0.245 meters. We will record every second pulse from two separate wheels, for redundancy and as a check on wheel slippage. This means that the traverse can be reconstructed in increments of about 0.5 m. These same wheel pulses and a gyro-stabilized compass provide the basic input to the Rover navigation computer which displays range, bearing, heading, and distance travelled to the astronaut. The bearing and heading are computed in increments of 1^{o} and the range and distance travelled are computed in increments of 100 meters. We will record the bearing every time it changes by $\pm 1^{o}$ (except in the immediate vicinity of the LM) and as a redundant check we will record the range in 100-meter increments. The range is computed using the third slowest wheel, so we will have a separate measure of the wheel slip and/or an internal range check at 100-meter increments. Finally, since there may be errors that will accumulate in both the range and bearing measurements we will use the known stop points to correct the traverse. Since these stops are likely to be in increments of one or two kilometers, we will have frequent updates to our traverse map. On the basis of this information we expect to be able to reconstruct the traverse to an accuracy of about 1% of the range and range differences over a few hundred meters to about 1 meter or better.

For the glacier tests, we have used a simple odometer circuit connected to one of the drive-wheels which generates signals every 1.5 meter. These are recorded independently on the tape recorder. These pulses have been used to determine the horizontal scale so that all the data discussed in this report have been plotted as field strength versus range.

Theoretical Work

We have previously reported on various aspects of the theory behind this experiment (Annan, 1972, Cooper, 1972, Sinha, 1972a, b, c) and have published a paper on some of the most preliminary glacier results, (Rossiter et al., 1972). We will not, therefore, review all these results in the present paper. Rather we will only summarize a few points which are pertinent to the data analysis.

The transmitting antennas are crossed dipoles; in the simplest case the traverses are run broadside to one dipole and off the end of the other. Using the geometry shown in Figure 2 this means Hz and H_ρ from the broadside antenna are both maximum-coupled and can be expected to show the interference patterns which are the basis of the experiment. Studies of the antenna patterns for these components show that the power above the surface is comparable to the power just below the surface so that significant interference between these two waves can be expected. In the case of the H_ϕ component off the end of the transmitter, however, power is transmitted above the surface but very little power is transmitted just below the surface. There is little interference, so this component is not as useful for determining the dielectric constant and loss tangent.

The other components (H_ϕ broadside and Hz and H_ρ endfire) are minimum-coupled to the respective transmitters. These components are consequently useful in looking for scattered energy reflected from either surface irregularities or subsurface inhomogeneities.

The antenna radiation pattern associated with these dipoles also contains a lobe which is pointed downwards at the critical angle as shown by Annan (1970) and by Cooper (1972). The lobe pattern is present in both

the broadside and endfire cases. The angle between the vertical and the peak of the lobe is given by $\sin \beta = \sqrt{\varepsilon_0/\varepsilon_1}$ where ε_0 is the dielectric constant of free space and ε_1 is the dielectric constant of the medium. In the case of ice where the ratio $\varepsilon_0/\varepsilon_1$ is given by 1/3.2 this angle is about 34^0. This energy does not appear at the surface unless there is a reflecting horizon at depth. In such a case the reflection appears at a distance $r = 2d \tan \beta$ where d is the depth of the reflector. For ice the depth to a reflector is given as $d \approx 0.8\ r$. In principle it is therefore possible to determine the dielectric constant and the loss tangent from the near-field interferences of the $H\rho$ and Hz components from the broadside antenna. Reflections can be studied by the $H\rho$ and Hz components from the broadside antenna and by the $H\phi$ component from the endfire antenna.

Athabasca Glacier Data

Most of our work to date has been concentrated on the Athabasca glacier in western Canada (Figure 4a). It is a well-studied glacier and is very accessible. Previous studies based on gravity (Kanasewich, 1963), seismology, drilling (Paterson and Savage, 1963) and electrical sounding (Keller and Frischknecht, 1961) have been made and a rough map of ice thickness is shown in Figure 4b. We have reported on earlier preliminary results (Rossiter et al., 1972) and in this paper restrict ourselves to one set of data taken in the summer of 1971 using a prototype of the flight equipment described earlier. The profile discussed is shown in Figure 4b and is marked by the transmitter at the southern end. The ice thickness is approximately 300 meters. The line was run from north to south and then repeated south to north with completely repeatable results.

The field strength data for all components at 4 mhz are shown in Figure 5 plotted as a logarithm of the power versus the distance in wavelengths. The length of the traverse was just over seven wavelengths at this frequency. Of particular interest and typical of all our runs at 4, 2 and 1 mhz is the fact that Hz and H_ρ from the broadside antenna and H_ϕ from the endfire antenna are large and smoothly varying functions. In particular the H_ϕ endfire component is very smooth showing almost no surface and subsurface wave interference. Hz broadside and H_ρ broadside, however, show sharp nulls. These nulls are the interferences generated from the surface, subsurface and reflected waves.

We have compared these field curves with sets of theoretical curves computed by the method of Annan (in press) and find that we can get surprisingly good determinations of the parameters,depth, dielectric constant and loss tangent at 4 mhz. We can also get good fits at 1 and 2 mhz although the uncertainties in the parameter determinations is greater (Table I). The minimum-coupled components (H_ρ and Hz endfire and H_ϕ broadside) however, show amplitudies that are 10 to 30 db below the maximum-coupled components at 1, 2 and 4 mhz (see Figure 5 for example) suggesting that scattering, although present, is not very significant.

At higher frequencies,scattering becomes more significant and at 32 mhz and at 16 mhz the only structure detectable is due to scattering. In Figure 7 a set of data of all three components from the E-W (broadside) transmitting antenna at 16 mhz is shown. The features to note in this plot are twofold. First, all components are about equal,suggesting that as much energy is scattered into the minimum-coupled H_ϕ component as is present in

the maximum-coupled H_ρ and Hz components. Second, is the erratic behavior of the field components, which show a wide range of rapid variations on a scale that is smaller than a wavelength. We conclude therefore that scattering is a dominant process at 16 mhz, important at 8 mhz and relatively unimportant at 4 mhz. This suggests that the distribution of scattering bodies ranges from about 35 meters to smaller sizes.

This seems to be a reasonable result based on the fact that this valley glacier is heavily crevassed and the typical size for the vertical and lateral extent of crevasses could be typically around 30 meters or less. These results are comparable to those found by Gudmandsen and Christensen (1968) who had trouble doing airborne radio sounding at 35 mhz over valley glaciers in West Greenland. They attribute this, at least in part, to the presence of crevasses in the valley glaciers.

Conclusions

The radio frequency interference technique developed for the Apollo lunar program is useful for measuring the dielectric constant and loss tangent of the upper layers of the moon in the frequency range from 1 mhz to 32 mhz. It will also be useful for detecting layering in the range from about 5 meters to a few kilometers, depending on the nature of the layers and of the electrical properties. In addition, it is likely to yield information on the presence of scattering bodies. These expected findings have been confirmed by tests over the Athabasca glacier. Here it was possible to measure the dielectric constant of ice as 3.3 and the loss tangent at 4 mhz as 0.10. The depth of the ice was estimated to be about 275 meters, a value in rough agreement with other determinations.

At 1 and 2 mhz the dielectric constant is about the same, as is the depth although the limits of uncertainty are larger. As seen in Table I the loss tangent of ice is roughly inversely proportional to frequency giving values of f. tan δ ranging from 0.20 to 0.40. There are only a small number of scatterers with dimensions less than about 35 meters, but there are larger numbers with smaller sizes.

Acknowledgements

We would like to acknowledge permission from the Jasper National Park authorities to work on the Athabasca glacier.

This work was conducted under NASA Contract No. NAS 9-11540.

	1 mhz			2 mhz			4 mhz		
	K	tan δ	Depth m.	K	tan δ	Depth m.	K	tan δ	Depth m.
Hz	$3.2 \pm .2$	$0.20 \pm .15$	230 ± 30	$3.3 \pm .1$	$0.16 \pm .01$	260 ± 10	3.3 ± 0.1	$0.1 \pm .01$	275 ± 5
Hp	NOT DIAGNOSTIC			$3.2 \pm .2$	$0.10 \pm .03$	270 ± 10*	3.3 ± 0.1	$.07 \pm .005$	275 ± 5

*Several other depths permissible

TABLE I

References

Annan, A. P., 1972, Radio interferometry depth sounding, part I - theoretical discussion, Geophysics, in press.

Annan, A. P., Radio interferometry depth sounding, Master of Science thesis, Department of Physics, University of Toronto, 1970.

Chung, D. H., Laboratory studies on seismic and electrical properties of the Moon, in press, the Moon.

Chung, D. H., W. B. Westphal and Gene Simmons, 1971, Dielectric behavior of lunar samples: Electromagnetic probing of the lunar interior, Proceedings of the Second Lunar Science Conference, Vol. 3, pp. 2381-2390, M.I.T. Press, Cambridge, Massachusetts.

Cooper, William W., TE/TM patterns of hertzian dipole in two- or three-layered medium, submitted for publication.

Evans, S., 1965, Dielectric properties of ice and snow - a review: J. Glaciol., v. 5, pp. 773-792.

Gudmandsen, P. and h. Lintz Christensen, Radioglaciology, interim report for EGIG of measurements in Greenland, May 1968, Laboratory of Electromagneti Theory, The Technical University of Denmark, Lyngby, D 77, October 1968.

Harrison, C. H., 1970, Reconstruction of subglacial relief from radio echo sounding records: Geophysics, v. 35, pp. 1099-1115.

Holser, W. b., R. J. S. Brown, F. A. Roberts, O. A. Fredriksson and R. R. Unterberger, 1970, Radio frequency propagation in salt domes 2. Pulse reflections from salt flanks: presented at SEG 40th Annual International Meeting, New Orleans.

Howard, H. L. and G. L. Tyler, Bistatic-radar investigation, Apollo 15 Preliminary Science Report, NASA SP 289, 1972.

Kanasewich, E. R., 1963, Gravity measurements of the Athabasca glacier, Alberta, Canada: J. Glaciol., v. 4, pp. 617-631.

Katsube, T. J. and L. S. Collett, 1971, Electrical properties of Apollo 11 and 12 lunar samples, Proceedings of the Second Lunar Science Conference, Vol. 3, pp. 2367-2379, M.I.T. Press, Cambridge, Massachusetts.

Keller, G. V. and F. C. Frischknecht, 1961, in Geology of the Arctic (International Symposium), edited by G. O. Raasch: Toronto, University of Toronto, v. 2, pp. 809-832.

Paterson, W. S. B. and J. C. Savage, 1963, Geometry and movement of the Athabasca glacier: J. Geophys. Res., v. 68, pp. 4513-4520.

Rinker, J. N. and S. J. Mock, Radar ice thickness profiles, Northwest Greenland, Special Report 103, U.S. Army Materiel Command, Cold Regions Research & Engineering Lab., Hanover, New Hampshire, May 1967.

Rossiter, J. R., A. P. Annan, G. A. LaTorraca, D. W. Strangway and G. Simmons, Radio interferometry depth sounding, part II - Experimental Results, Geophysics, in press.

Saint-Amant, M. and David W. Strangway, 1970, Dielectric properties of dry, geologic materials: Geophysics, v. 35, pp. 624-645.

Sinha, Ajit K., Fields from a horizontal electric dipole over a lossy dielectric medium and its applications in the radio-interferometry method, part I - The half-space, submitted for publication, Geophysics.

Sinha, Ajit K., Fields from a horizontal electric dipole over a lossy dielectric medium and its application in the radio-interferometry method, part II - Layer over a perfect reflector, submitted for publication, Geophysics.

Sinha, Ajit K., Fields from a horizontal electric dipole over a lossy dielectric medium and its applications in the radio-interferometry method, part III - Layer over an arbitrary reflector, submitted for publication, Geophysics.

Strangway, D. W., 1969, Moon: Electrical properties of the uppermost layers: Science, v. 165, pp. 1012-1013.

Strangway, D. W., G. R. Olhoeft, W. B. Chapman and J. Carnes, Electrical properties of lunar soil - dependence on frequency, temperature and moisture, Geophysics, submitted for publication.

Unterberger, R. R., W. T. Holser and R. J. S. Brown, 1970, Radio frequency propagation in salt domes 1. Theory, laboratory and field measurements of attenuation: presented at SEG 40th Annual International Meeting, New Orleans.

Figure Captions

1. Attenuation distance as a function of frequency from lunar samples and from remote lunar sensing.

   Straight lines show theoretical values for typical dielectrics which have a loss tangent which is independent of frequency.

   1) Weaver (1965) - thermal emission and radar observations
   2) Tyler (1968) - bistatic radar
   3) Chung et al (1971) - lunar igneous sample 12002
   4) Collett and Katsube (1971) - lunar breccia sample 10065
   5) Collett and Katsube (1971) - lunar fines sample 10084
   6) Gold et al., (1971) - lunar fines
   7) Strangway et al., (in press) - lunar fines

2. Sketch illustrating operation of surface electrical properties experiment and various waves expected to be transmitted through and above lunar surface.

3. Sketch showing sequence of transmitted frequencies and sequence of transmitting and receiving antennas. Two frames marked OFF are used to monitor the background external noise at all frequencies in three successive frames, and to measure the internal noise with input shorted and looking in succession at two calibrated noise diodes. The frame marked cal. is used for synchronizing transmitter and receiver and to record the internal temperature.

4. a) Location map of the Athabasca glacier

   b) Sketch map of the Athabasca glacier, showing the location of the profile discussed in this report. Contours are the generalized thicknesses as determined from previous drilling and seismic studies.

5. Complete set of data at 4 mhz showing $H\rho$, $H\phi$ and Hz from both the E-W (broadside) and the N-S (endfire) antenna.
   a) E-W transmitter, Hz
   b) E-W transmitter, $H\phi$
   c) E-W transmitter, $H\rho$
   d) N-S transmitter, Hz
   e) N-S transmitter, $H\phi$
   f) N-S transmitter, $H\rho$
6. $H\rho$ and Hz components from E-W antenna (broadside) showing field data and theoretical fits (upper curve). Parameters correspond to those in Table I.
   a) $H\rho$ component - 4 mhz
   b) Hz component - 4 mhz
   c) $H\rho$ component - 2 mhz
   d) Hz component - 2 mhz
   e) $H\rho$ component - 1 mhz
   f) Hz component - 1 mhz
7. Typical set of data taken at 16 mhz to illustrate scattering effect of glacier. All components Hz, $H\phi$ and $H\rho$ from the E-W transmitter (broadside) are about equal.

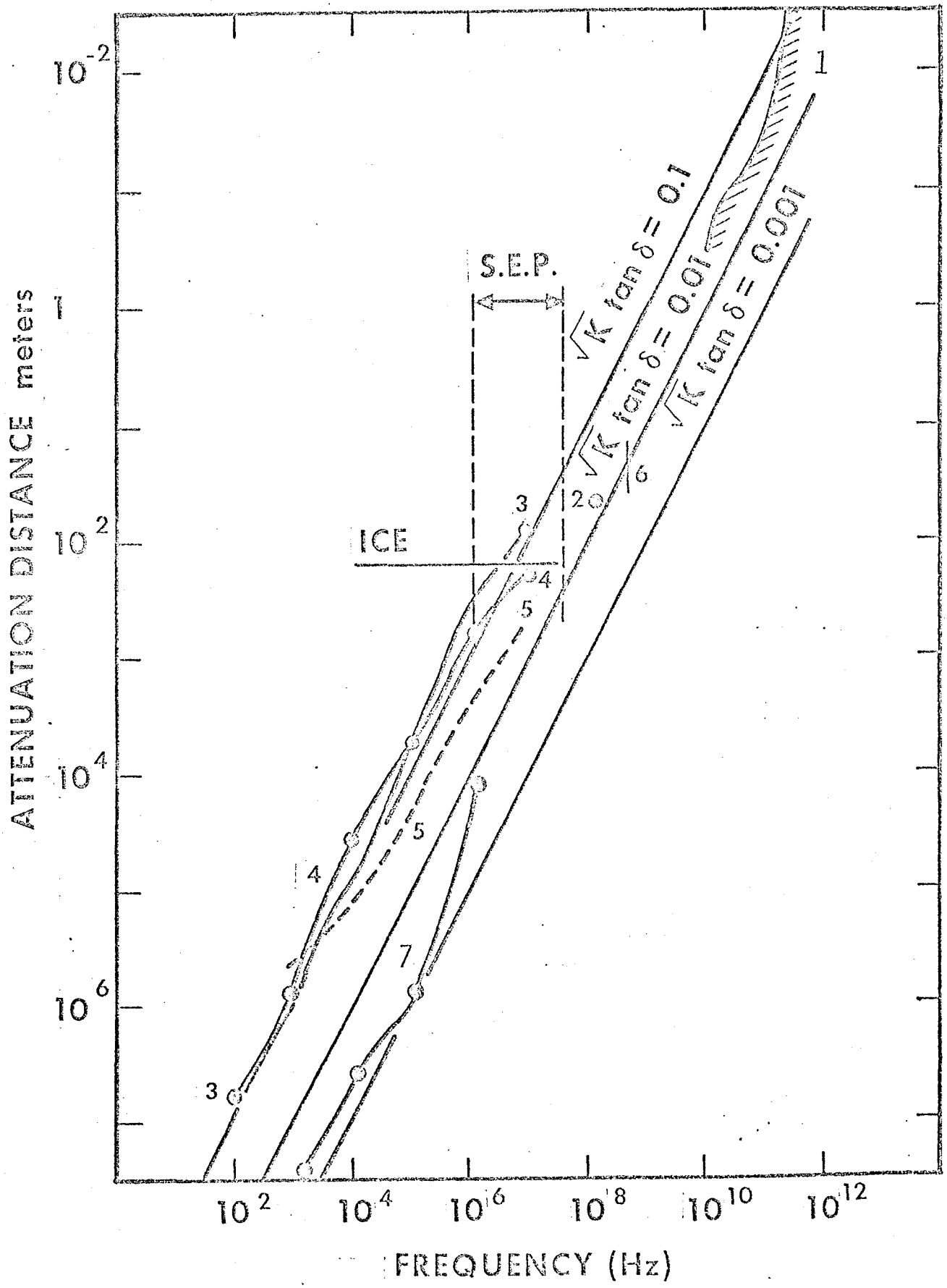
ATTENUATION DISTANCE meters
10^{-2}
1
10^{2}
10^{4}
10^{6}
S.E.P.
ICE
$\sqrt{K \tan \delta} = 0.1$
$\sqrt{K \tan \delta} = 0.01$
$\sqrt{K \tan \delta} = 0.001$
1
2
3
4
5
6
7
10^{2}
10^{4}
10^{6}
10^{8}
10^{10}
10^{12}
FREQUENCY (Hz)

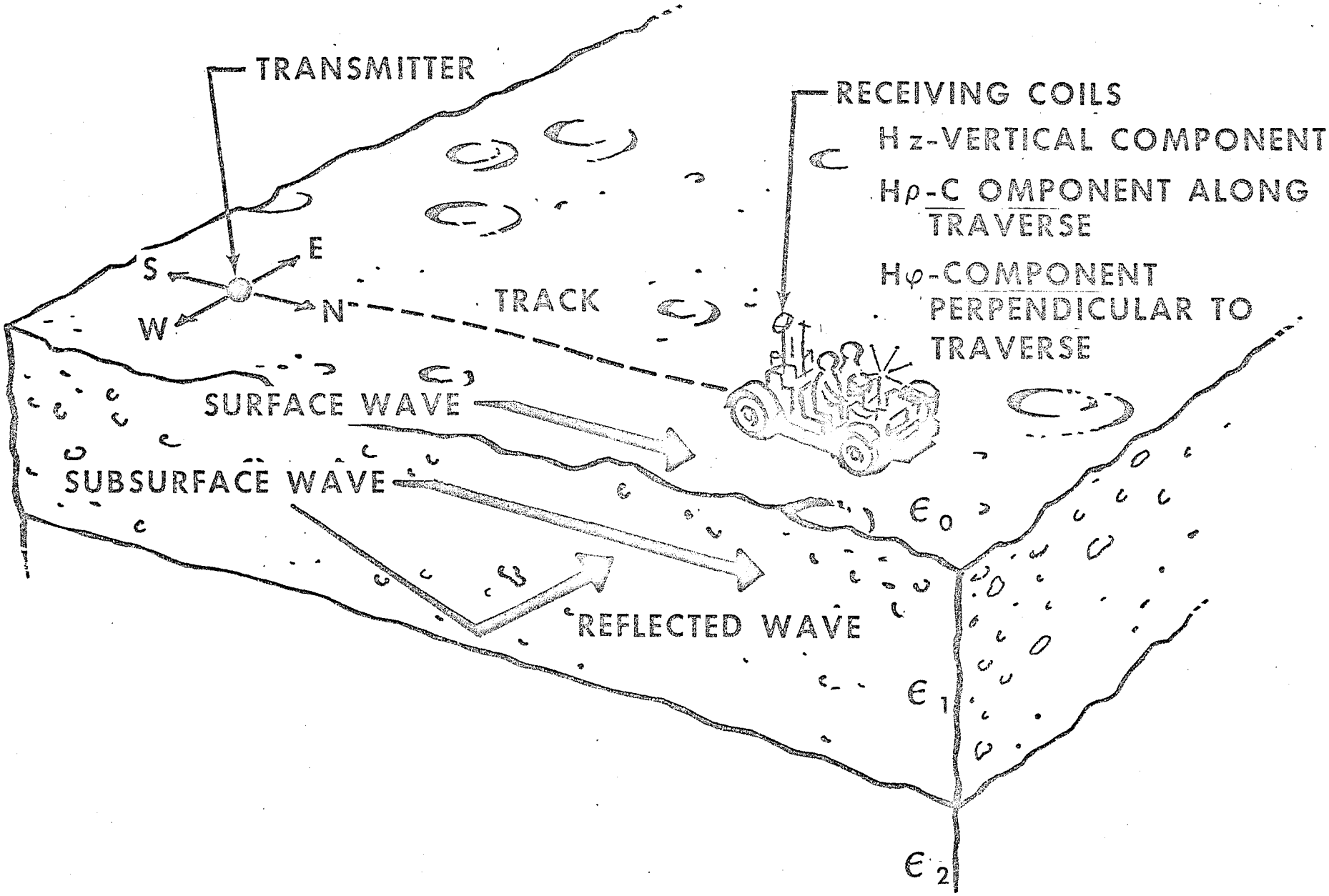
TRANSMITTER
RECEIVING COILS
Hz-VERTICAL COMPONENT
Hρ-C OMPONENT ALONG TRAVERSE
Hφ-COMPONENT PERPENDICULAR TO TRAVERSE
S
E
W
N
TRACK
SURFACE WAVE
SUBSURFACE WAVE
REFLECTED WAVE
ϵ_0
ϵ_1
ϵ_2

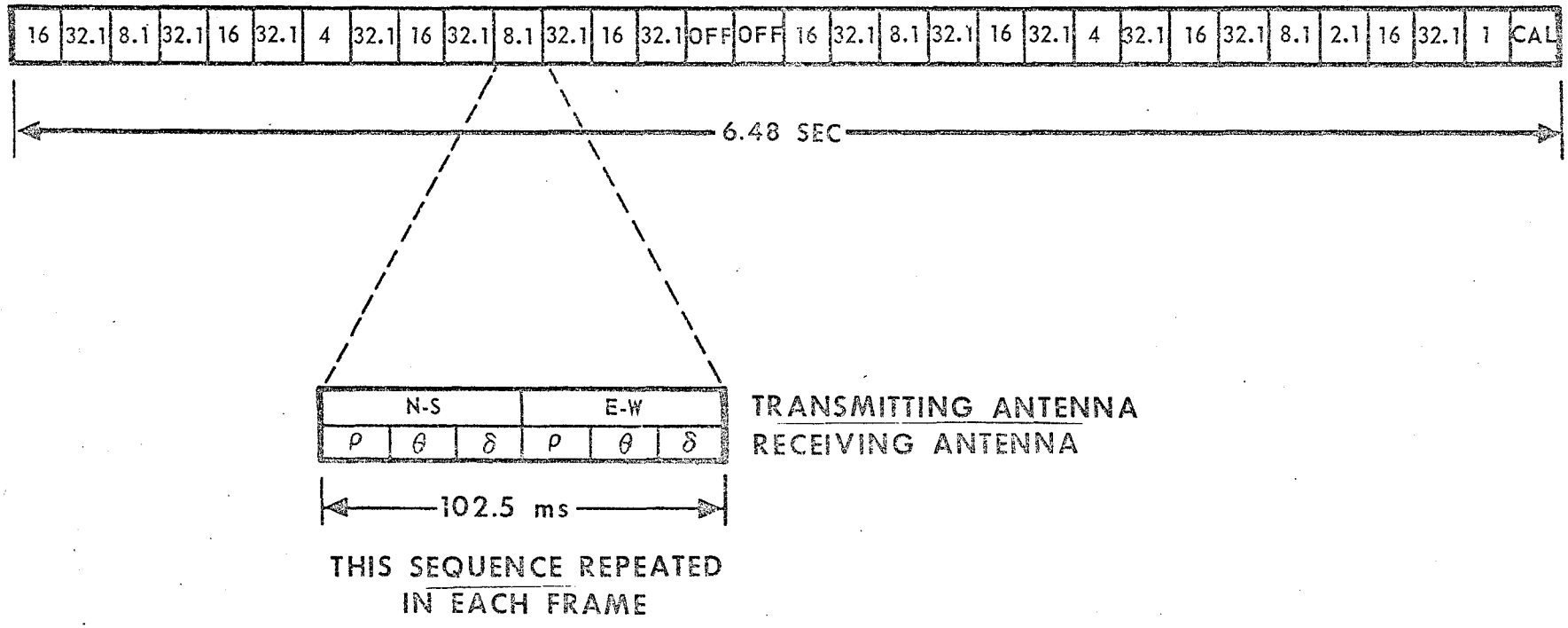
16 32.1 8.1 32.1 16 32.1 4 32.1 16 32.1 8.1 32.1 16 32.1 OFF OFF 16 32.1 8.1 32.1 16 32.1 4 32.1 16 32.1 8.1 2.1 16 32.1 1 CAL
6.48 SEC
N-S
E-W
ρ θ δ ρ θ δ
102.5 ms
TRANSMITTING ANTENNA
RECEIVING ANTENNA
THIS SEQUENCE REPEATED IN EACH FRAME

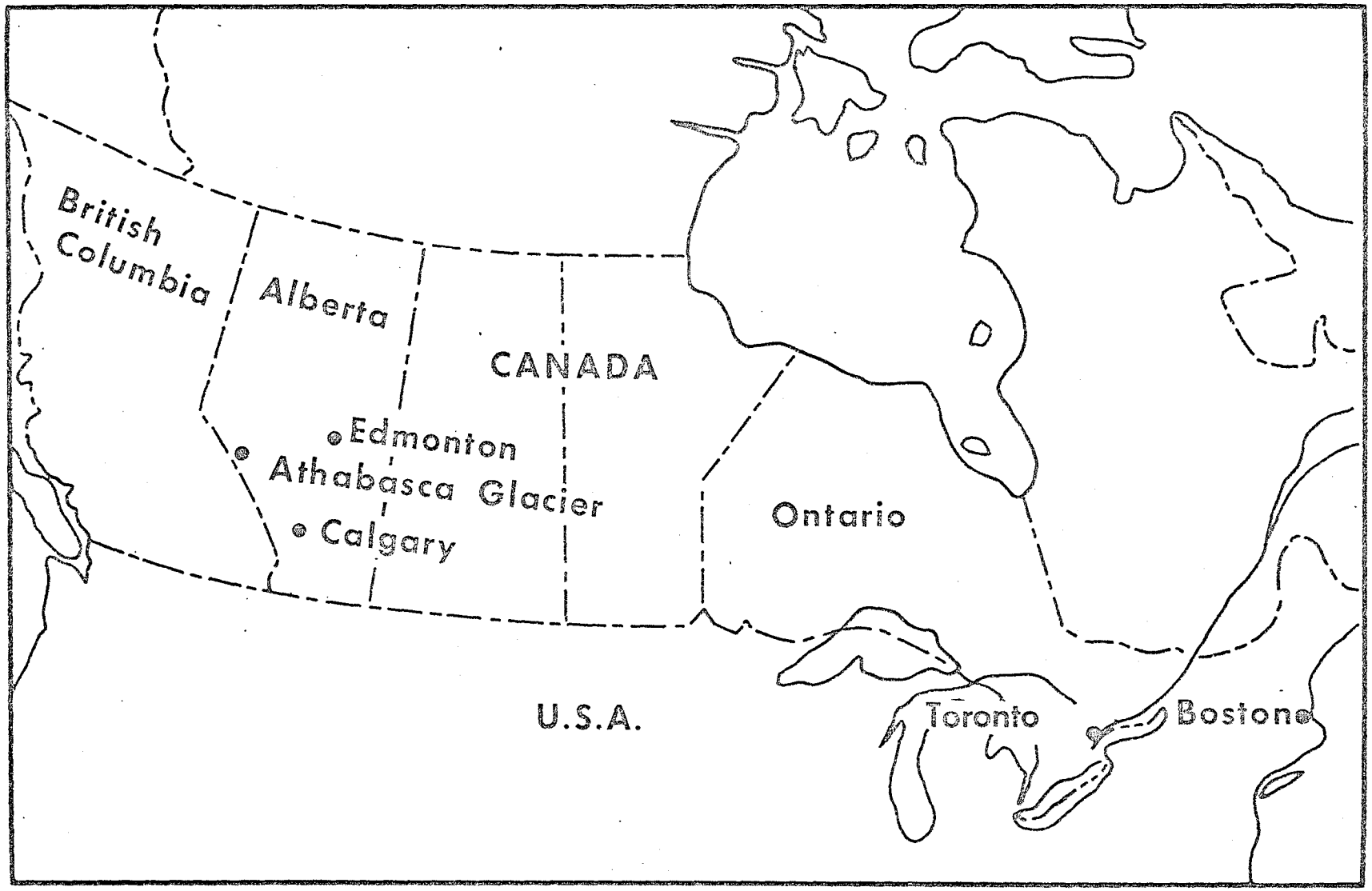

GENERAL LOCATION MAP

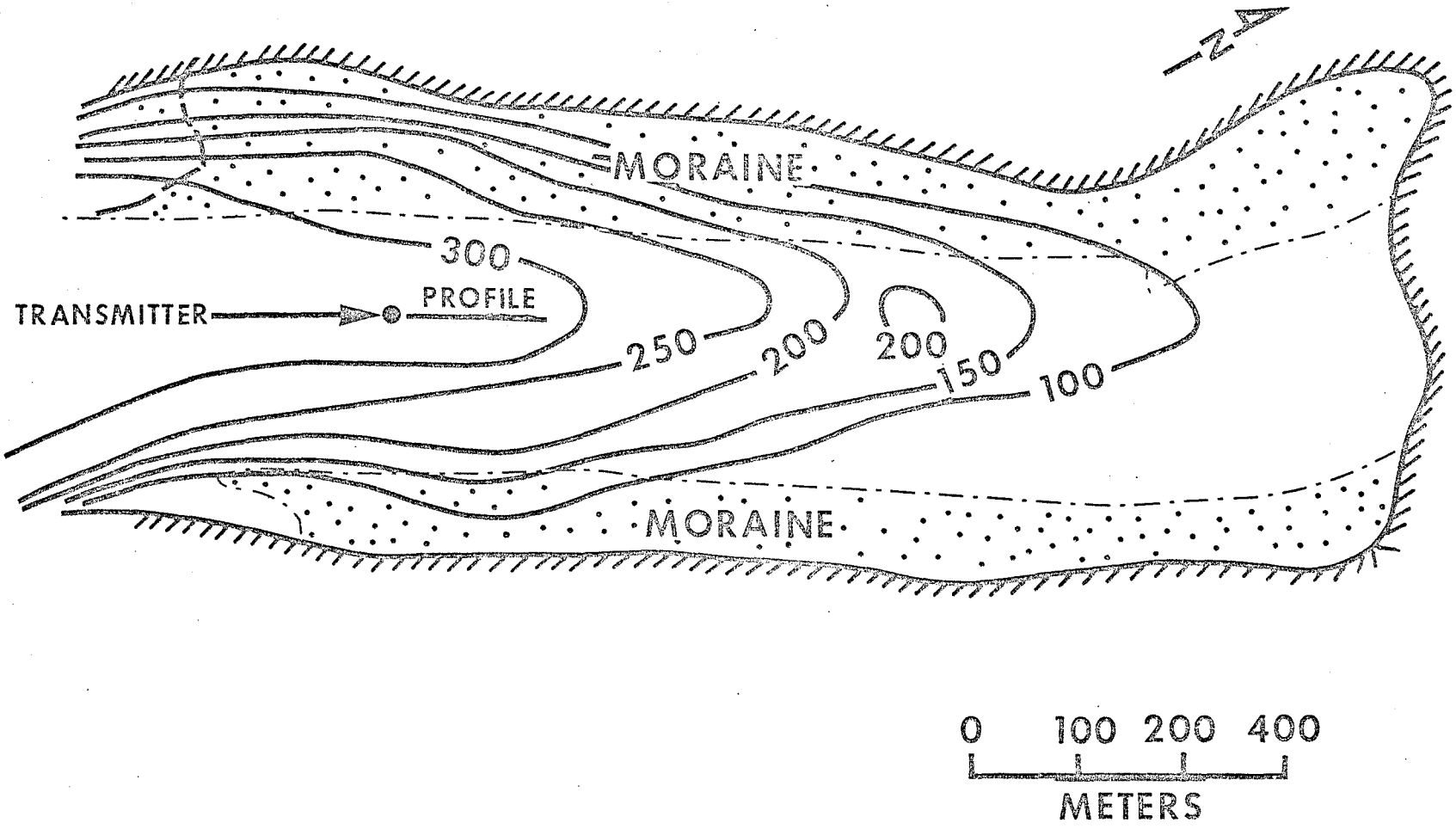
N
MORAINE
300
TRANSMITTER
PROFILE
250
200
200
150
100
MORAINE
0 100 200 400
METERS

4b

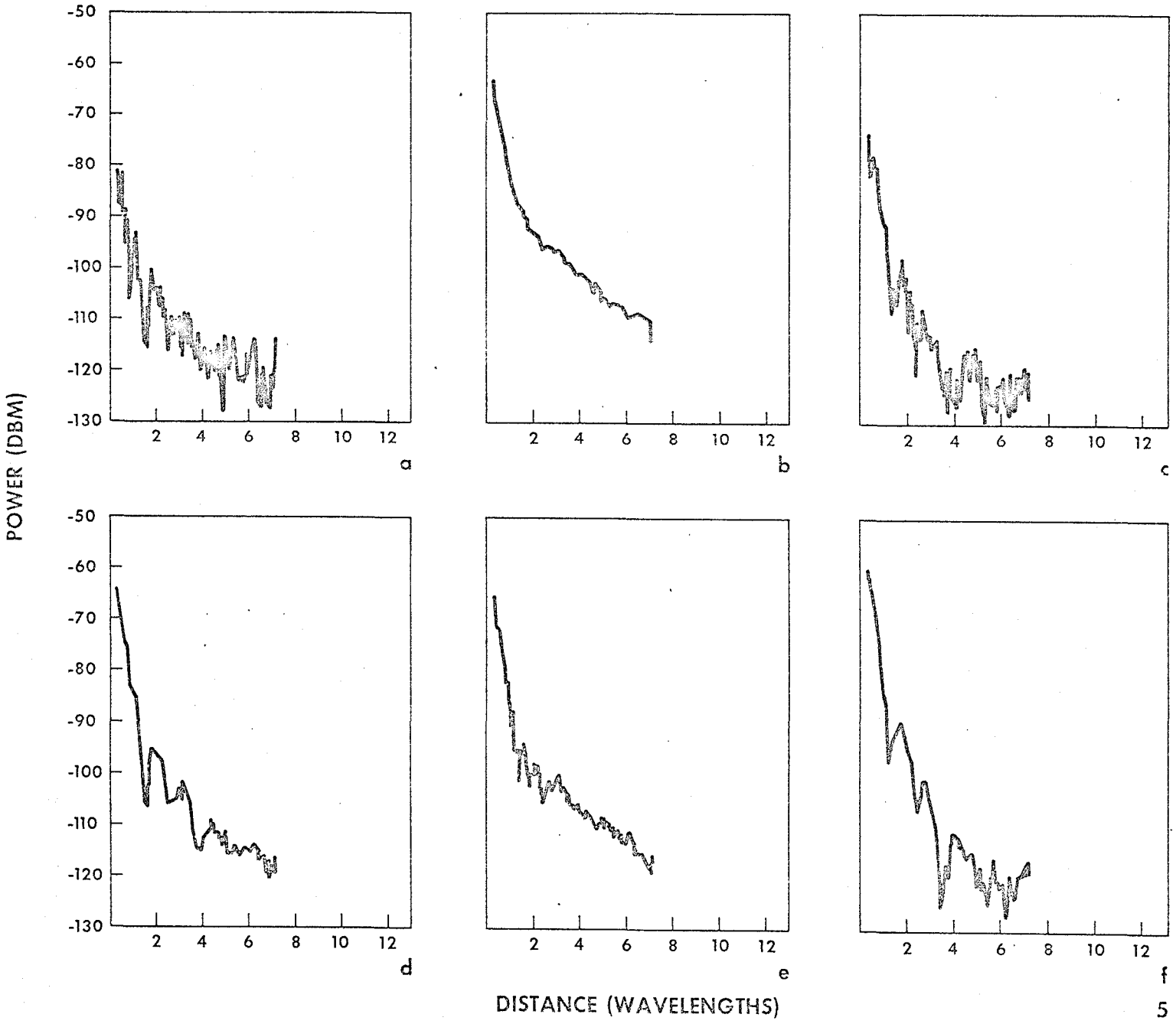
POWER (DBM)
-50
-60
-70
-80
-90
-100
-110
-120
-130
2
4
6
8
10
12
a
b
c
d
e
f
DISTANCE (WAVELENGTHS)

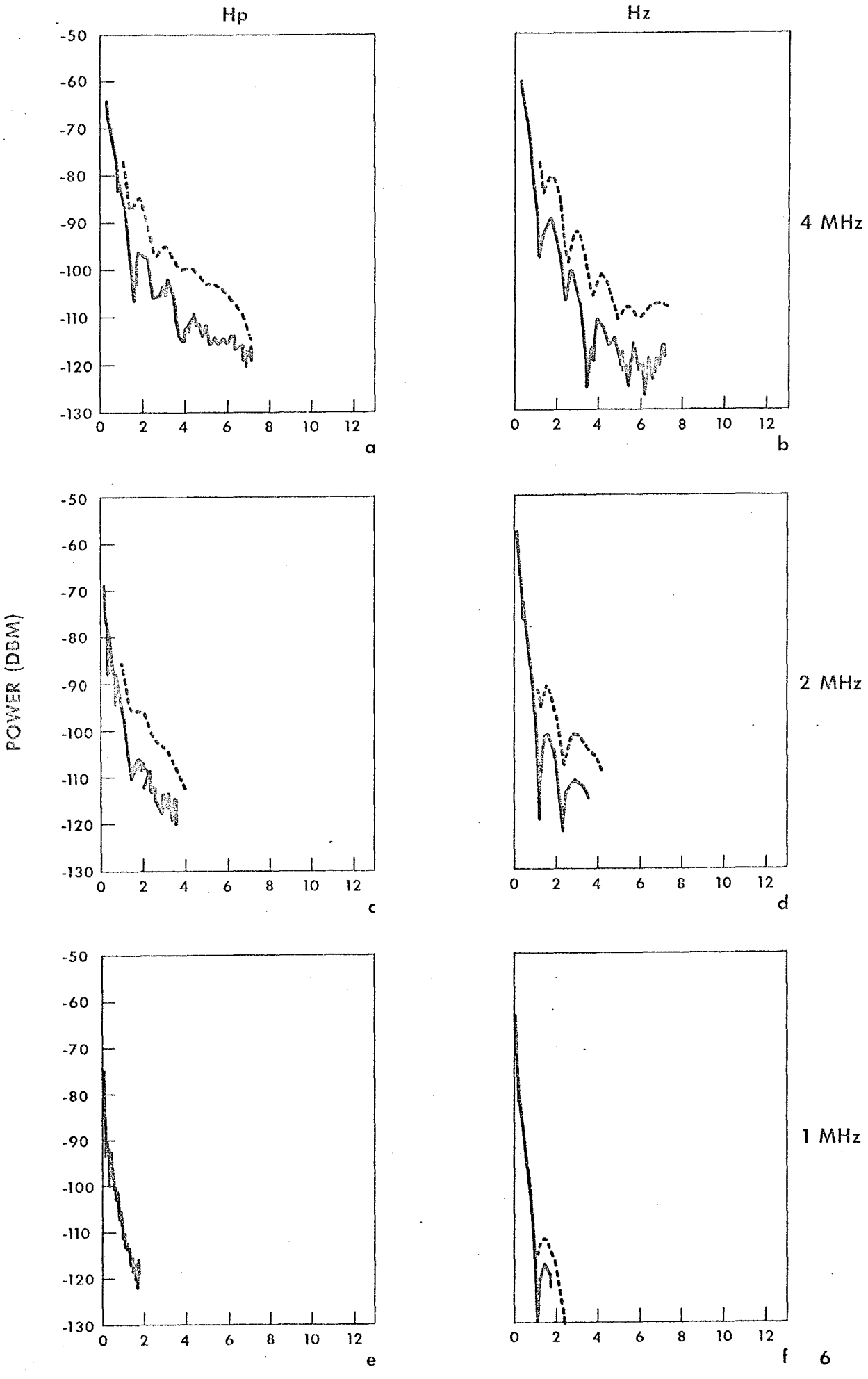
Hp
Hz
POWER (DBM)
-50
-60
-70
-80
-90
-100
-110
-120
-130
0
2
4
6
8
10
12
a
b
c
d
e
f
4 MHz
2 MHz
1 MHz

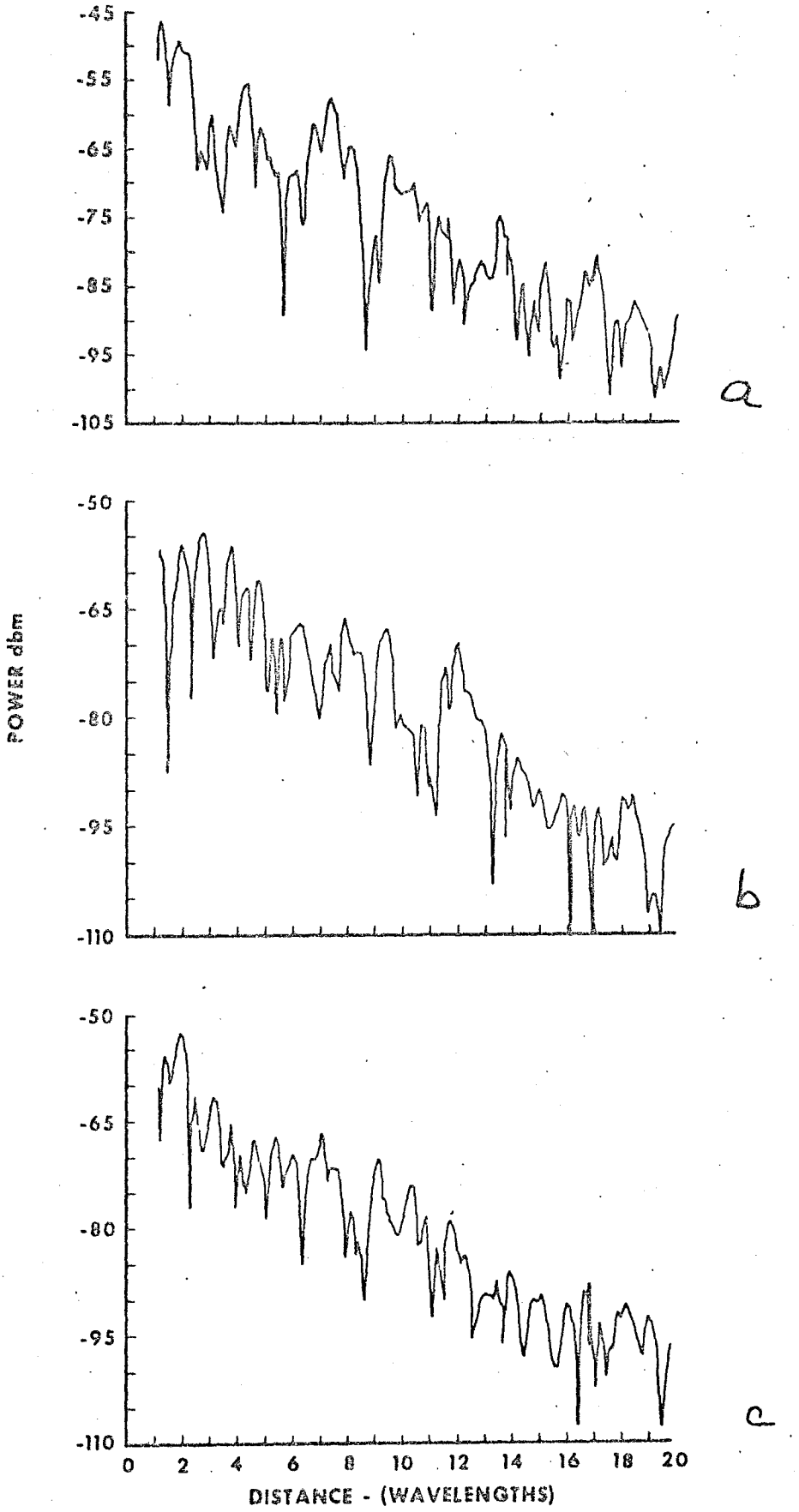
-45
-55
-65
-75
-85
-95
-105
a
-50
-65
-80
-95
-110
b
POWER dbm
-50
-65
-80
-95
-110
c
0
2
4
6
8
10
12
14
16
18
20
DISTANCE - (WAVELENGTHS)